

Evaluation of a Novel Thermobrachytherapy Seed for Concurrent Administration of Brachytherapy and Magnetically Mediated Hyperthermia in Treatment of Solid Tumors

Parsai E. I.*, Gautam B., Shvydka D.

Abstract

Concurrent hyperthermia and radiation therapy in treatment of cancer show a strong evidence of a synergistic enhancement. We designed a new self-regulating Thermo-Brachytherapy seed, which serves as a source of both radiation and heat for concurrent administration of brachytherapy and hyperthermia. The Thermo-Brachytherapy seed has a core of ferromagnetic material which produces heat when subjected to alternating electro-magnetic (EM) field and effectively shuts off after reaching the Curie temperature (T_c) of the ferromagnetic material thus realizing the temperature self-regulation. For the thermal characteristics, we considered a model consisting of one seed as well as an array of 16 seeds placed in the central region of a cylindrical water phantom. Isodose distributions from Iodine-125 source of these models were computed using MCNP5 Monte Carlo simulation technique. The modeling for the isothermal distribution computations performed using a finite-element partial differential equation solver package COMSOL Multiphysics. It is shown that by changing frequency and intensity of the alternating applied magnetic field, we can obtain desired isothermal distribution within the target volume. Adjustment of these two parameters allows one to match the desired isosurface dose distribution with an optimized isothermal distribution achieving optimal treatment in both modalities. We also demonstrate that the effect of tissue cooling down due to the blood perfusion could be compensated by adjusting the externally applied magnetic field parameters. In this paper, parameters effecting radiation and thermal distribution on this proposed new seed will be presented.

Keywords

Hyperthermia, Brachytherapy, Ferromagnetic Induction Heating, Blood Perfusion

Introduction

A treatment modality for cancer where the temperature of cancer tissue is elevated from normal to a critical temperature is known as hyperthermia. This is often an adjuvant treatment offered in conjunction with radiation or chemo therapy. The critical temperature for this therapeutic effect ranges from 42-46 °C for a specified period of time; usually 30 to 60 min. Temperature values within this range are not directly harmful to normal cells, while malignant ones are destroyed as they are more sensitive to high temperatures. Heat causes several subtle changes in tissue physiology such as increased blood perfusion, vascular permeability, and metabolic activity. Protein damage is the main molecular event underlying the biological effects of hyperthermia in the tem-

University of Toledo
Medical Center,
3000 Arlington Avenue,
Toledo, Ohio 43614
USA.

*Corresponding author:
E. Ishmael Parsai, Ph.D.,
DABR, FAAPM, FACRO
Professor & Director
Univ. of Toledo Graduate
Medical Physics Pro-
grams
Chief, Division of Medi-
cal Physics
Department of Radiation
Oncology
Mail Stop 1151
3000 Arlington Avenue
Toledo, Ohio 43614-
2598
Voice: +1-419-383-4541
Fax: +1-419-383-3040
E-mail: e.parsai@uto-
ledo.edu

perature range of 39 to 42° C [1]. The studies have shown that the protein denaturation is the most likely thermal effect causing permanent irreversible cell killing [2]. A variety of methods have been developed to induce temperature rises either locally in selected regions of specific organs or over the whole body [3-7]. The currently available modalities of hyperthermia are often limited by deficiencies in tumor targeting ability and the resultant tissue temperature distribution for deep seated tumors [8-10]. Electromagnetic induction heating of a ferromagnetic implant has been used to heat a small volume of deep seated tissue. This type of implant serves as a self regulating source of heat if the ferromagnetic material of appropriate Curie temperature is used. The inductively heated implants have certain conceptual advantages. They offer relative ease of the heat delivery and adjustment in the thermal dose distribution. The temperature in the region of interest can be controlled via external field parameters (intensity and frequency of the magnetic field) and no invasive thermometry is needed [11].

It has been shown that the hyperthermia not only kills the cancerous cells but also sensitizes them to other treatment modalities such as radiation therapy and chemotherapy.

A number of clinical trials have been performed comparing the effect of hyperthermia along and in combination with external beam radiation therapy. The results show significant improvement in both tumor control and survival rate without considerable increase in side effects [12-16]. For the best radiation sensitization, the time interval between the administrations of the both modalities has to be within an hour.

One of the preferred radiation treatment methods for the deep seated solid tumors such as prostate cancer is the brachytherapy via permanent seed implant. In this method seeds containing the radioactive isotope of low energy and relatively short half-life are inserted inside the cancerous tissue under ul-

trasound guidance. A limited number of studies performed for the concurrent hyperthermia and interstitial brachytherapy shows this approach to be very effective [17]. We propose a

Thermo-Brachytherap seed capable of delivery of heat and radiation concurrently to deep seated solid tumors. The seed consists of a ferromagnetic Ni-Cu alloy core covered with radioactive isotope Iodine-125, and sealed in a tungsten shell, thus offering a simultaneous source of radiation and heat via ferromagnetic induction heating process. The proposed design features self regulation of the temperature in the range near the Curie point of the ferromagnetic material. Furthermore, it addresses some of the shortcomings of other hyperthermia methods, such as, achieving better temperature uniformity through a more appropriate placement of the seeds, avoiding complex invasive thermometry and feedback loops. In this article we report the summary of results of the dosimetric and thermal properties of the proposed seed as well as the effect of the tissue blood perfusion on the thermal distribution within the target area.

Materials and Methods

Seed Design: The Thermo-Brachytherap seed is based on one of the standard iodine seed implants BEST seed model 2301, I-125. The schematic of the Thermo- Brachytherapy seed is presented in Fig.1. It retains the same double layer of titanium encapsulation and external dimensions (length and diameter) allowing relative ease of the prototype implementation from the manufacturing standpoint. The core

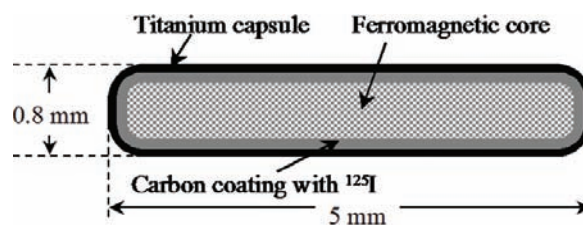


Figure 1: Sketch of the Thermo-Brachytherapy seed

of the seed is made up of ferromagnetic Ni-Cu alloy having diameter of 0.44 mm and physical length of 4.64 mm. The ferromagnetic core is coated with a 0.08 mm thick layer of an organic carbon layer impregnated with I-125 similar to the standard seed design. The modification in the internal structure is necessary to accommodate proper heat conduction and maximize the heating power of the seed.

Monte Carlo Simulation Method: Radiation characteristic parameters were estimated using a Version 5 of the Monte Carlo N-Particle code (MCNP5). All simulations were operated in the photon and electron transport mode (Mode: p,e) in the MCNP5 code so that both primary photons and resulting secondary electrons were properly transported. The energy cut off was set to 5keV for both photons and electrons. The photon interaction cross-section data used in this study was the P04 library distributed by the Radiation Shielding Information Computing Center [18].

The energy spectrum for the ^{125}I source was taken from the AAPM TG-43U report [19]. For Monte Carlo simulations, a seed was positioned at the center of a 30 cm diameter spherical water phantom. The long axis of the source has been chosen as the z -axis in Cartesian coordinates (which coincides with the polar axis in polar coordinates) and the y -axis along the transverse bisector. At low photon energies, absorbed dose to water can be approximated by collision kerma [20]. For the determination of dosimetric parameters, absorbed dose to water was scored using an MCNP F6:p tally feature at radii ranging from 0.3 to 10.0 cm along the transverse axis and at angles ranging from 0° to 180° in 5° bins. The MCNP5 F6 tally calculates the energy absorbed per gram of material comprising each tally volume. The number of photon histories needed to achieve simulation results with accuracy better than 3% was between 1×10^6 and 1×10^{10} . The dose calculation formalism proposed by AAPM Task Group 43 has been followed to calculate the radiation characteristics air kerma strength, dose rate

constant, geometry function, radial dose function, and anisotropy function of this proposed seed. [21]

Thermal Properties: Thermal distribution from the ferromagnetic induction heating process can be divided in two parts: induction of eddy and hysteretic currents in the ferromagnetic core under alternating electromagnetic field, and transfer of the induced heat from the core to the surrounding medium.

A system of two equations, the Ampere's law for vector potential \vec{A} and the Penn's Bio heat equation, were the governing equations for the thermal distribution calculation. The equations are expressed as

$$(i\omega\sigma - \omega^2\varepsilon)\vec{A} + \nabla \times (\mu^{-1}\nabla \times \vec{A}) = \vec{J}^e \quad (i)$$

$$\rho C_p \frac{\partial T}{\partial t} - \nabla \cdot k \nabla T = Q(T, \vec{A}) + M_b - W_b C_b (T - T_a) \quad (ii)$$

Here, time average of the inductive heating over one period $Q = \frac{1}{2} \sigma |\vec{E}|^2$, \vec{J}^e external current density, ω is frequency, σ - electric conductivity, ε and μ - electric permittivity and magnetic permeability, ρ - density, T - temperature, C_p - specific heat capacity of the medium, k - its thermal conductivity, M_b - is the metabolic heat generation in the tissue. The last terms on the right hand side of equation (ii) describe blood flow where C_b is the specific heat of blood, W_b the volumetric blood perfusion of the tissue, T_a the temperature of the arterial blood entering the volume. For the first approximation we ignore the blood flow contribution to the heat conduction and drop the last two terms in equation (ii). The effects of the blood perfusion on the thermal distribution were studied for the blood perfusion rate (W_b) of 0.0009, 0.0017, 0.0025 and 0.0035/s.

In order to evaluate thermal distribution of the heat induced in the ferromagnetic core of the proposed seed a modeling study was performed using a finite-element analysis method.

A typical model layout for the evaluation of thermal properties and the temperature distribution is shown in Fig. 2, where a single seed is located in the central region of a cylindrical

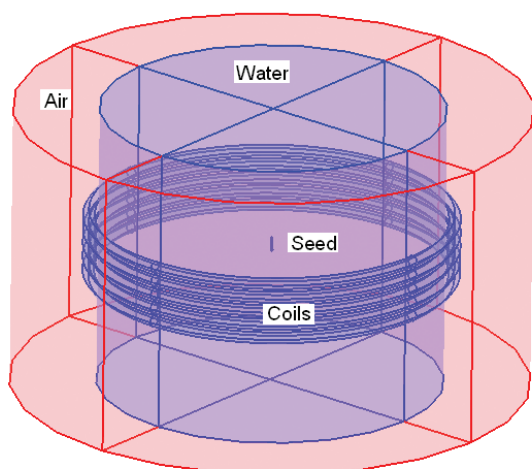


Figure 2: A Model layout for the thermal properties and temperature distribution with a seed in the water phantom.

cally shaped water phantom (diameter 12 cm) surrounded by air. Five induction coils (cross-sectional diameter 0.4 cm) are wrapped around the phantom and the seed is placed parallel to the magnetic field vector. To get better temperature coverage over a bigger volume we put 16 seeds separated by a distance of 1 cm (not shown in figure) in the form of 4x4 rectangular array, at the mid-plane of the phantom. Temperature dependent magnetic permeability for ferromagnetic Ni (70.4%) - Cu (29.6%) alloy was used and the system was solved for the frequencies of 75 - 200 kHz and magnetic field values at the middle of the phantom (H_0) of 200-550 Oersteds (Oe). One Oe is 79.578 ampere per meter which is approximately = 1 Gauss. The following boundary conditions were set to solve the model problem. Initial reference temperature of the water phantom was set to the normal body tissue temperature 37°C and the temperature of the surrounding air was set to be 22 °C. All the boundaries of the air medium outside the phantom were set to be at thermal insulation and the water air interface was set to flow heat continuously.

A finite-element partial differential equation solver package COMSOL Multiphysics (Heat transfer model and the AC/DC module) was used to model the thermal properties and the

3-D temperature distributions. We employed the transient analysis type for heat transfer and time harmonic analysis for the induction current in time dependent segregated solver. The simulations are performed with time stems of 1 minute or less for up to total time of 30 minutes with the relative solution tolerance of 0.01 and absolute tolerance of 0.001.

Results

Radiation Characteristics

Monte Carlo output was obtained as an energy deposition per unit mass (MeV/g) and then converted to dose rates. The dose rate at a point $P(r, \theta)$ at the radial distance r , and the polar angle θ , from a cylindrically symmetric line source centered at the origin of the water phantom, was used to calculate the dose rate constant, the radial dose function, and the anisotropy function. The direct comparison with data previously published on the standard BEST 2301 is made for every calculated TG-43 parameter [22].

Air-kerma strength (S_k) and Dose rate constant (Λ): The Monte Carlo output for the air-kerma rate was calculated to be $K^{MC}(d, 90^\circ) = 9.438 \times 10^{-06}$ MeV/g photon or, converted to conventional units, $K^{MC}(d, 90^\circ) = 2.973 \times 10^{-02}$ cGy mCi $^{-1}$ h $^{-1}$. This resulted in the value of the air kerma strength $S_k = 0.742 \pm 0.009$ U mCi $^{-1}$.

The Monte Carlo output for the dose rate at 1cm along the transverse direction is computed as 2.192×10^{-4} MeV/g. This gives the dose rate constant value $\Lambda = 0.930 \pm 0.018$ cGy h $^{-1}$ U $^{-1}$.

The dose rate constant for the Thermo-Brachytherapy is about 8% less than the dose rate constant of the Best® Model 2301 ^{125}I seed, (1.01 cGy h $^{-1}$ U $^{-1}$), calculated through Monte Carlo by Sowards *et. al.*

Radial dose function $g(r)$: The radial dose functions, $g(r)$, derived from Monte Carlo simulations are presented in the Fig. 3. This figure also shows the comparison of the radial dose functions of Thermo-Brachytherapy and

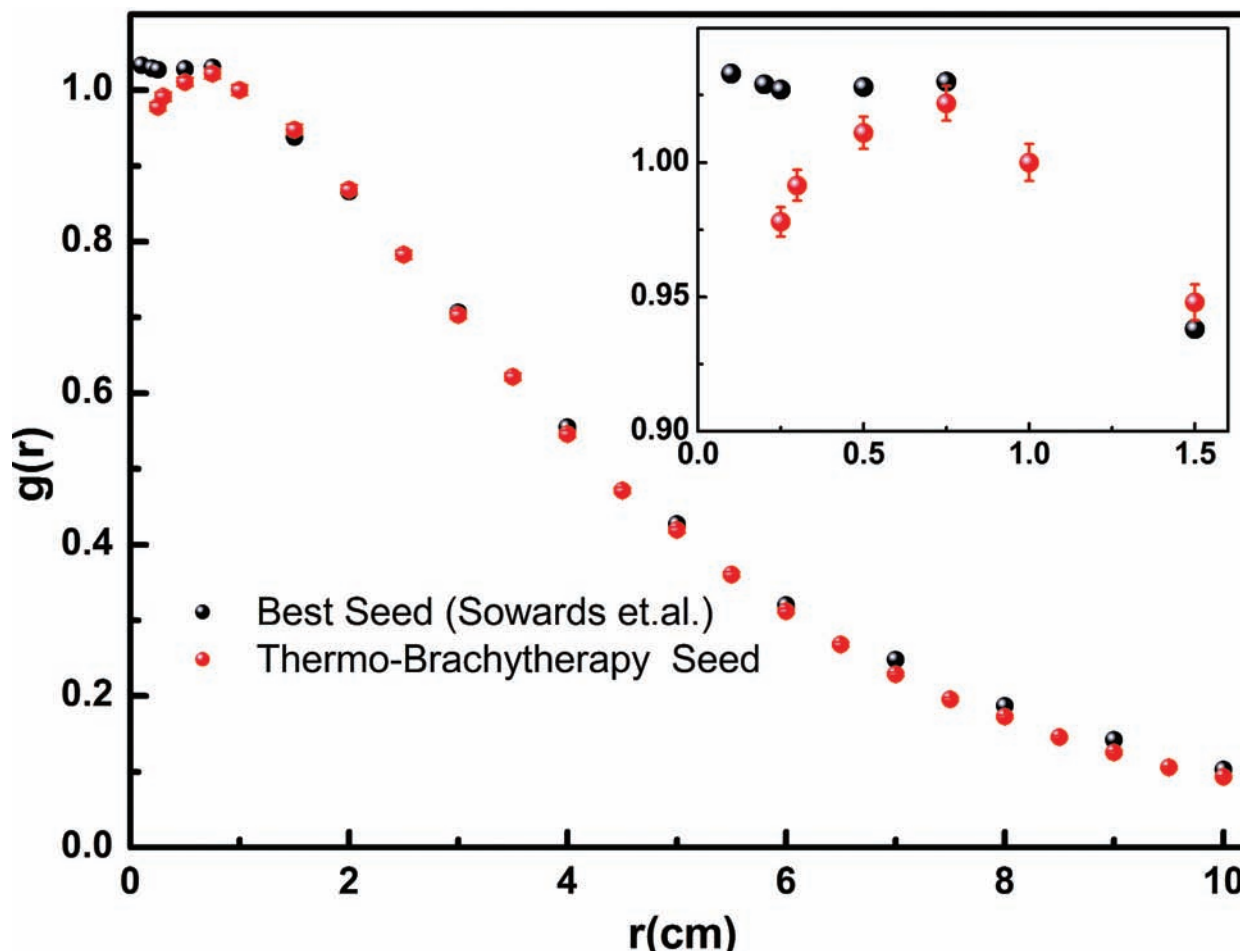


Figure 3: Radial dose function $g(r)$ for the Thermo-Brachytherapy seed and the BEST 125I, Model (Sowards et. al)

the Best[®] Model 2301 ¹²⁵I seeds. The data indicates a good agreement (within 1%) between the two values for most of the radial distances. Our calculated radial dose data for the Thermo-Brachytherapy seed matches favorably with published $g(r)$ data for Best[®] Model 2301 ¹²⁵I seed except for the small radial distance ($r < 1$ cm). One can appreciate (see inset of Figure 3) the deviation of $g(r)$ values for the Thermo-Brachytherapy seed from that of the Best[®] Model 2301 ¹²⁵I. In the new seed the radial function increases with increase of the radial distance up to 0.75cm. It has its highest value at the distance of 0.75 cm and then it starts decreasing. On the other hand the radial dose function for Best[®] Model 2301 ¹²⁵I seed stays more or less constant for the radial distance up to 0.75 cm and then decreases.

The calculated radial dose function is fitted

to a fifth order polynomial function as follows:

$$g(r) = a_0 + a_1r + a_2r^2 + a_3r^3 + a_4r^4 + a_5r^5 \quad (10)$$

where, $a_0=0.9584$, $a_1=0.1635$, $a_2= -0.1555$, $a_3=0.0319$, $a_4=-0.0028$, and $a_5=-9.231 \times 10^{-5}$ respectively.

Anisotropy Functions $F(r, \theta)$: Figure 4 shows the comparisons of the $F(r, \theta)$ values for the Thermo-Brachytherapy seed with that of Best[®] Model 2301 ¹²⁵I seed for radial distances of 1 and 5 cm. Anisotropy function for the Thermo-Brachytherapy seed slightly deviates from anisotropy functions of Best[®] Model 2301 ¹²⁵I seed. The $F(r, \theta)$ value decreases with increase of the angle (θ) and reaches at the minimum value around at an angle in between 10 to 15° and again starts increasing to become unity at the transverse direction ($\theta=90^\circ$). The

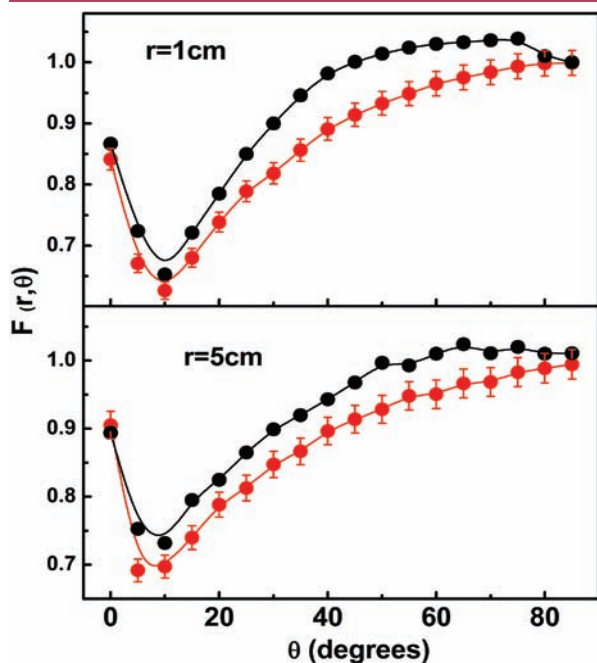


Figure 4: Comparison of 2-D Anisotropy function $F(r, \theta)$ between the Thermo-Brachytherapy seed and the BEST ^{125}I Model seed (Sowards et. al), at a radial distance 1 and 5cm.

minimum value of $F(r, \theta)$ increases with increase of radial distance. The variation between anisotropy functions of the Thermo-Brachytherapy seed and Best[®] Model 2301 ^{125}I

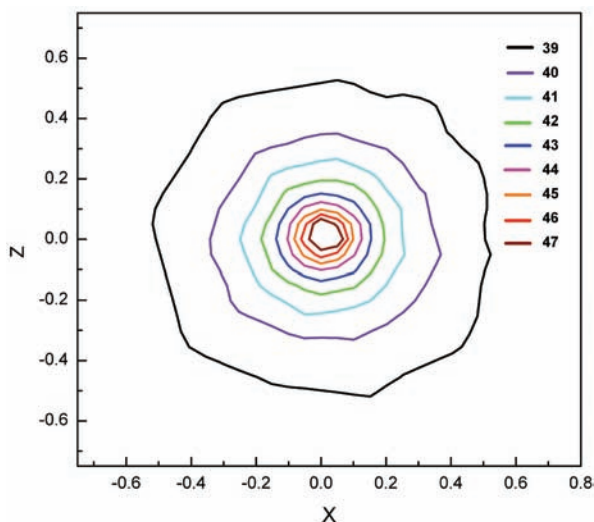


Figure 5: Temperature distribution profiles of the seed bisector cross-sectional plane by a single seed heating at magnetic field intensity (H_0) 300 Oe and frequency (f) 150 kHz.

therapy seed is about 8% less than that of Best[®] Model 2301 ^{125}I seed (0.98).

Thermal Properties and Temperature Distribution

A cross sectional view of the temperature distribution due to a single seed along the seed bisector plane for magnetic field $H_0 = 400$ Oe and frequency 150kHz is shown in Fig 5. The result provides the general trend of spatial variation of the temperature due to one seed. The data shows that the highest temperature is observed near the seed surface and the temperature decreases as we move away from the seed. At the surface of the seed the temperature is about 47°C , dropping to 42°C and 39°C at the distances of 2 mm and 5 mm respectively from the seed surface. Clearly, only a very small fraction of the volume between the seeds heats above the therapeutic temperature range ($T \leq 42^\circ\text{C}$).

Figure 6 shows time dependent temperature variation for the seed surface and the middle point of the phantom with time. The seed surface temperature rises rapidly and reaches to about 48°C within a minute after the magnetic field is turned on. After that the temperature stays almost constant throughout the entire time. Figure 6 also presents the data for the power produced by the seed. One can see that when the field is turned on the Thermo-Brachytherapy seeds starts thermal power production. As the temperature of the seed core increases, approaching the Curie temperature, the thermal power produced by the seed decreases.

Adequate thermal coverage of an extended volume of tissue requires a large number of Thermo-Brachytherapy seeds. We used 16 thermal seeds to heat a hypothetical target. For this seed configuration, higher temperature is found (data is not shown here) around the middle of the volume as compared to the region around the peripheral of the delineated target. In this hypothetical example our aim was to show that by achieving an ideal seed

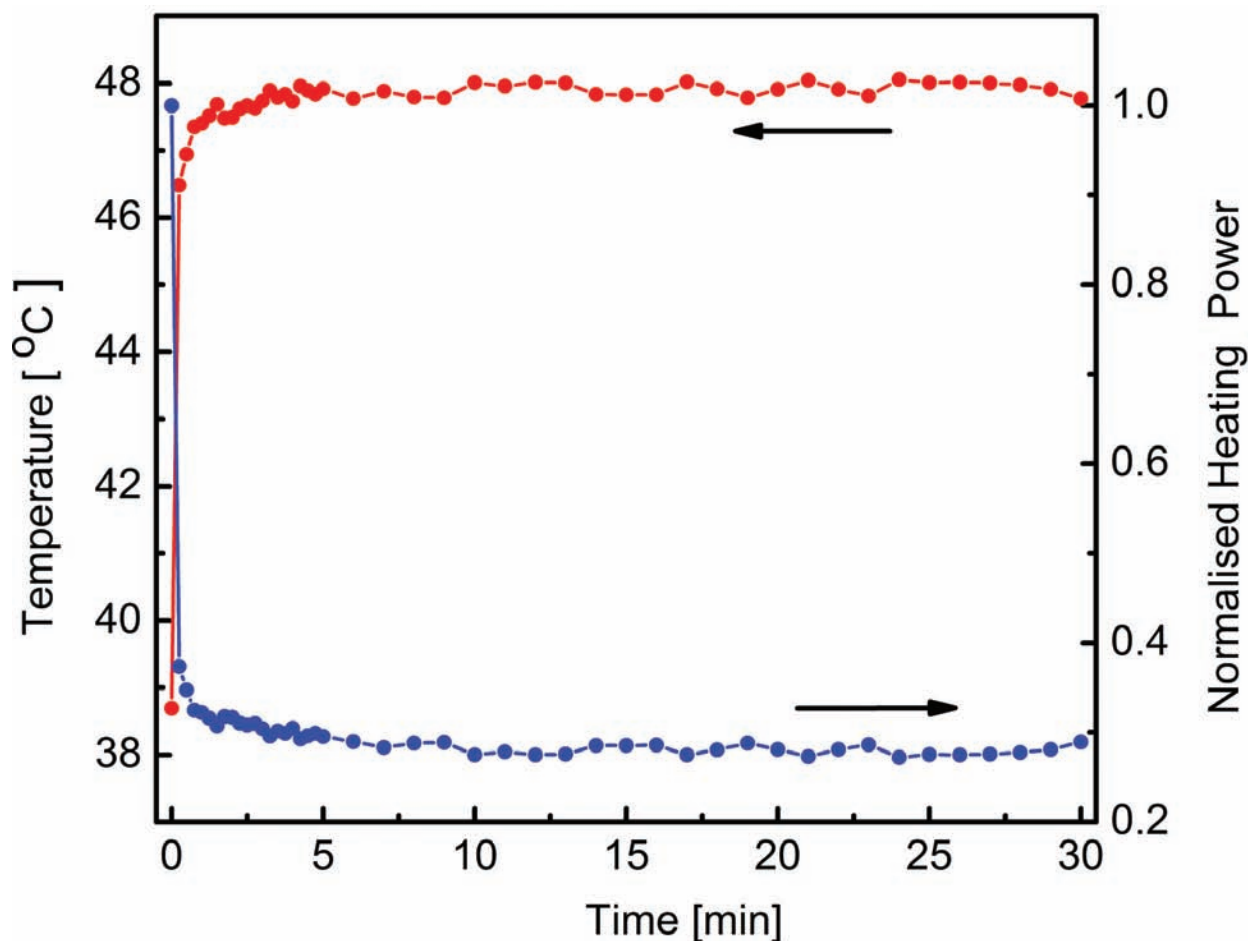


Figure 6: Variation of temperature at the seed surface and the heating power of a Thermo-Brachytherapy seed.

implant for optimized dose distribution, one can adjust the thermal parameters of the seed to achieve an optimized thermal distribution to effectively heat the delineated target volume as seen in figure 7.

To alter the temperature distribution within the targeted volume and attain a better coverage we can change variables such as intensity (H_0) and the frequency (f) of magnetic field. Figure 7 presents the comparison of temperature distribution for fixed magnetic field strength of 300 Oe and varying frequency. Figure 7(a) shows the cross sectional isothermal surfaces for the frequency of 75 kHz. Clearly, only a very small fraction of the volume between the seeds heats above the therapeutic temperature range ($T \leq 42^\circ\text{C}$). For this set of variables, most of the volume is under-heated, exhibiting islands of “cold” spots. The data for

magnetic field $H_0 = 300$ Oe and frequency 100 [Figure 7(b)] show most of the volume around the seed distribution heated up to the therapeutic temperature range ($T > 42$). From Fig 7(b), one can also see that only the 40°C isothermal surfaces cover the entire seed configuration whereas the 42°C isothermal surface missed some volume around the corner seed. For the frequency of 125 kHz [see Figure 7(c)], the larger volume is covered by the therapeutic temperature range: the 42°C isothermal surface covers the whole seeds volume around. The better temperature coverage over larger volume was obtained for this condition but there are some hot spots in areas near the seed surfaces. For the frequency of 150 kHz [see Figure 7(d)], even a higher temperature coverage over larger volume is achieved but there is a large fraction of the volume near seed

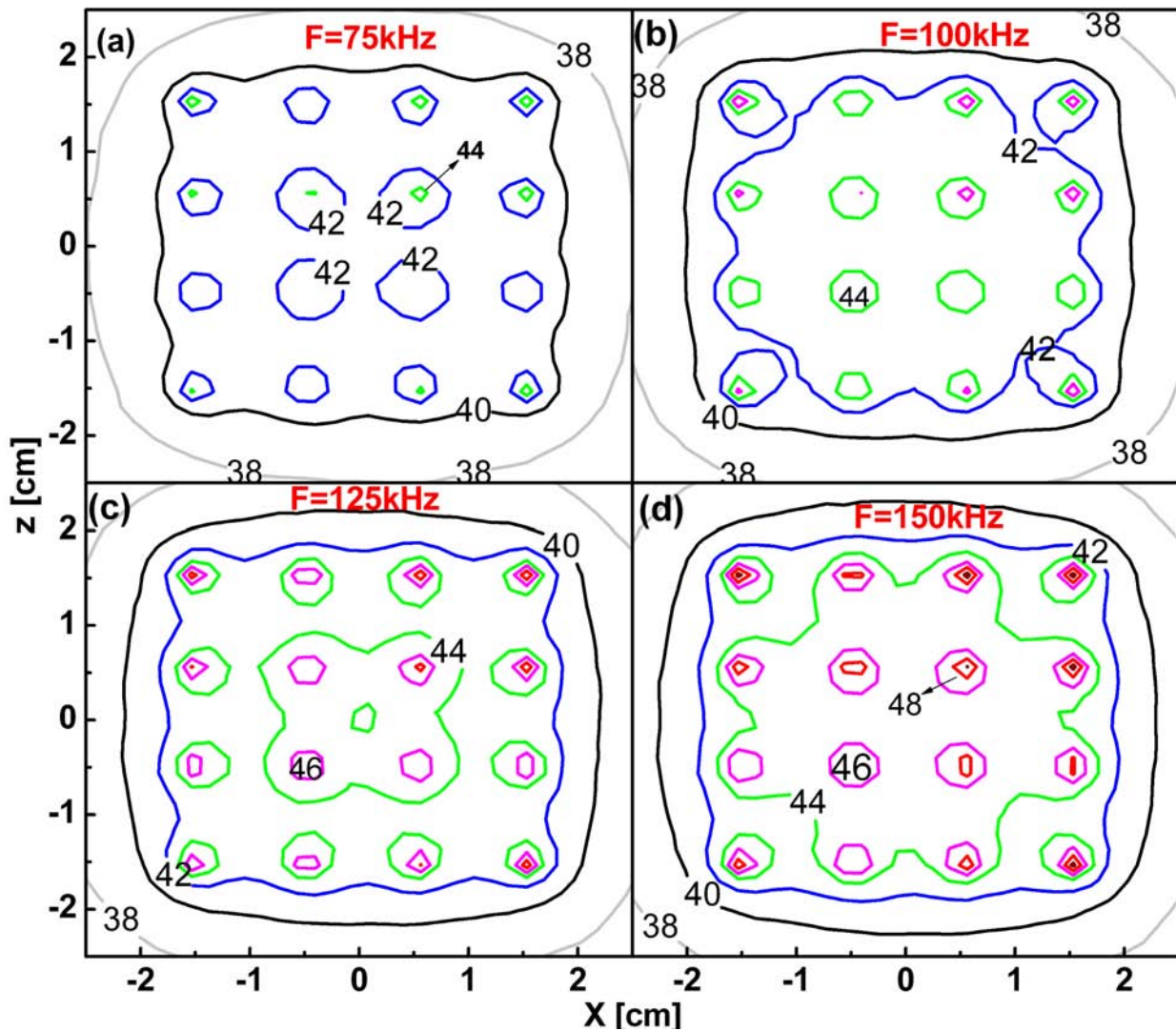


Figure 7: Cross sectional Isothermal profiles for magnetic field strength of 300 Oe and frequency (a) 75 kHz (b) 100 kHz (c) 125 kHz (d) 150 kHz.

surfaces being overheated. As in the case of the treatment planning for radiation dose distribution, achieving the best isothermal distribution requires optimization of placement of the seeds, adjustment of intensity (H_0) and the frequency (f) of the magnetic field.

A comparison of the isothermal distribution and the radiation isodose distribution produced by the Thermo-Brachytherapy seed is performed. Figure 8 presents the comparison results of the radiation isodose and the isothermal distributions ($f=125$ kHz and $H_0=300$ Oe) for the 4x4 square arrays of seeds in a hypothetical target. The radiation dose is prescribed as 160cGy at the periphery of the target vol-

ume. The isothermal distribution for magnetic field values $f=125$ kHz and $H_0=300$ Oe shows the similar coverage as the radiation isodose distribution. One can also see that the 42°C isothermal distribution almost perfectly overlaps with the 100% radiation isodose distribution. This indicates that one can easily get the desired isothermal distribution over the certain target volume by changing the magnetic field variables (frequency and the intensity) to match with the ideal radiation dose distribution.

In the realistic patient where a target volume is to receive a given dose, the blood perfusion rate affects the thermal distribution patterns.

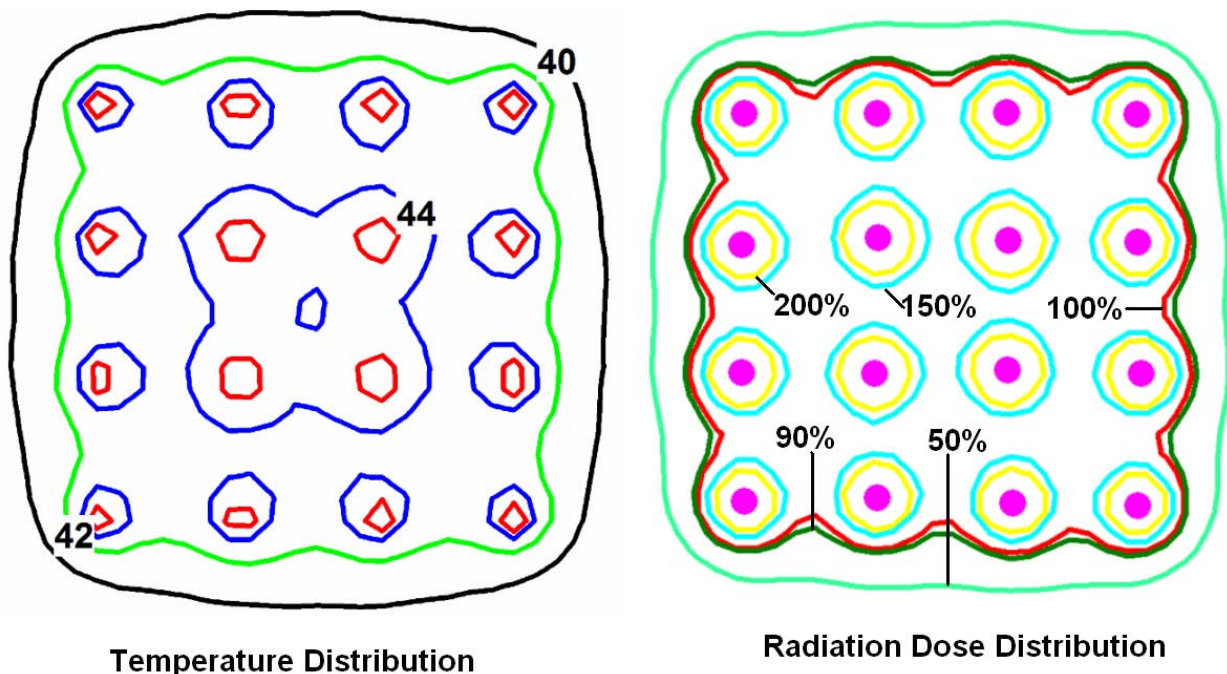


Figure 8: Comparison of cross sectional radiation dose distribution and temperature distribution ($f= 125$ kHz and $H_0=300$) profiles.

To account for the effect of blood perfusion, a uniform blood perfusion rate was assumed and the modeling study was performed. The data presented in Fig 9 shows the thermal distribution patterns in the uniform blood perfusion rate of 0.0025/s. Figure 9(a) shows the cross sectional isothermal surfaces for the frequency of 150 kHz and magnetic field of 300 Oe. Only 40°C isothermal surface covers the volume of the entire seed configuration. A very small region near the seed heats above the therapeutic temperature range ($T \leq 42^\circ\text{C}$). For this set of variables, the power generated by the seed is not enough to overcome the heat taken out by the blood perfusion. To compensate the effect of the blood flow one needs to increase either the intensity or the frequency of magnetic field or both. The data for magnetic field $H_0=300$ Oe and frequency 200 [Figure 9(b)] show most of the volume around the seed distribution heated up to the therapeutic temperature range ($T > 42$). From Fig 9(b), one can see that the entire seed volume covered by the 42°C isothermal surfaces. For the field intensity of 550 Oe and 200 kHz frequency [see Figure 9(d)], better temperature coverage is achieved

and only a small fraction of the volume near seed surfaces being overheated.

Discussions

The calculated radiation characteristic parameter values such as dose rate constant, radial dose function and anisotropy function of the Thermo-Brachytherapy seed are only slightly different from those of the Best® Model 2301 ^{125}I seed. The deviation of these values for the new seed from those of the Best® Model 2301 ^{125}I seed is most likely due to the removal of the air gap and redistribution of the I-125 source inside the seed. Even though the thickness of the source is kept the same as in the Best® Model 2301 ^{125}I , the removal of the air gap and redistribution of the Iodine-125 source and change in the effective length of the source results in different air kerma strength and the dose distribution around the seed.

The single seed heating data shows that the region close to the seed surface gets very good temperature coverage and as the distance from the seed surface increases the temperature drops rapidly. The rapid drop of the temper-

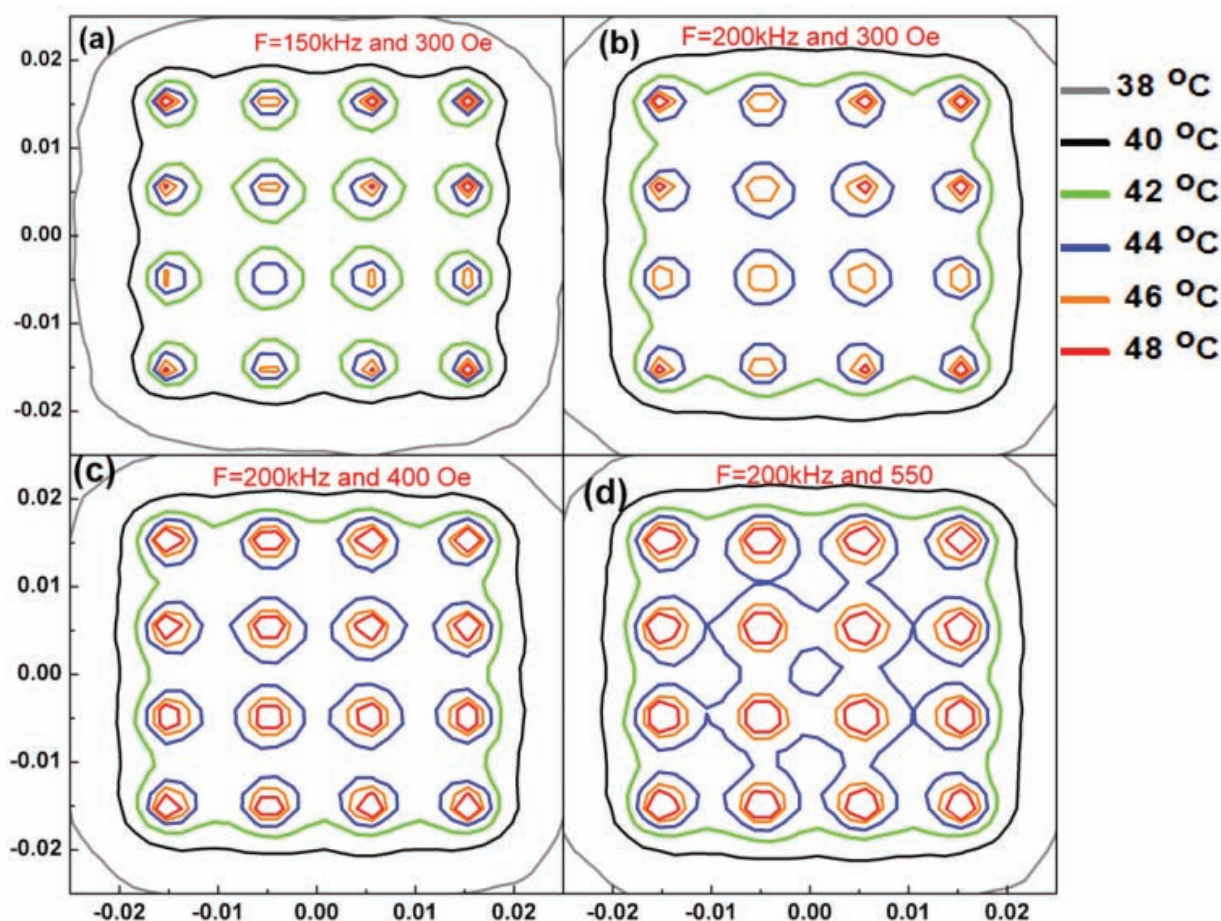


Figure 9: Cross sectional Isothermal profiles at blood perfusion rate of 0.0025 s^{-1} for different magnetic field parameters

ature with increasing distance from the seed surface allows heating the tissue selectively. In an ideal therapy, the normal structures near the target should get the minimum possible radiation and thermal dose. Seeds are implanted in the target tissue to irradiate and to heat the cancerous cells. During the treatment the target is heated to the therapeutic temperature range while the surrounding normal tissues stay at the temperature close to normal body temperature.

For a hyperthermia treatment to be practical the initial temperature rise after the EM field is turned on has to be reasonably short. The data of the induction heating of the Thermo-Brachytherapy shows that seed surface temperature rises rapidly and stays constant around the Curie temperature (T_c) of the ferromagnetic material used. The temperature

control mechanism at the temperature around the T_c of the ferromagnetic core is explained as follows. As soon as the magnetic field is turned on, eddy current is produced on the surface of the ferromagnetic core due to the electromagnetic induction. The resistive heating of the induced current produces heat rapidly. This causes the rapid rise on the temperature of the ferromagnetic core. As the temperature of the core rises gradually and reaches to the T_c of the Ni-Cu alloy the relative magnetic permeability decreases gradually and reaches unity. The decrease of the relative permeability decreases the production of the thermal power in the ferromagnetic core. As a result, the temperature starts decreasing and the magnetic permeability starts increasing. The increase in permeability starts increasing the thermal power production in the ferromagnetic core.

The T_c of the alloy can be altered by changing the composition of the constituent elements of the alloy. This property allows one to set the T_c according to desired level to get the more uniform temperature distribution throughout the volume of interest.

As in the case of the treatment planning for radiation dose distribution, achieving the best isothermal distribution requires optimization of placement of the seeds, adjustment of intensity (H_0) and the frequency (f) of the magnetic field. In case of the treatment using the Thermo-Brachytherapy seed, the alteration of the seed position can change both the radiation and the thermal distribution patterns. Therefore the only option to maximize the temperature coverage within the target volume in a real seed implant case, is to optimize the seed positions for an ideal radiation dose coverage, then by adjustment of the magnetic field parameters such as frequency and the field intensity achieve ideal thermal distribution coverage. Once the target volume is defined and the prescribed radiation dose is planned using the treatment planning system for the radiation, the temperature dose also can be prescribed over the target volume and planned using the thermal dose planning system, or employing software packages such as COMSOL to determine the best field parameters to heat the seeds. One can easily get the desired isothermal distribution over the certain target volume by changing the magnetic field variables (frequency and the intensity) to match with the ideal radiation dose distribution.

Adding the complexity of blood flow in a real patient and how does that effect removal of heat to the targeted area, one realizes that the temperature distribution would be different when the blood flow is taken into consideration. In such case, heat may be exchanged through the walls of the arterial and venous blood vessels. For example, a venous flow passing through a higher temperature region can absorb heat and transfer it to a relatively cooler nearby region. This effect will not be

important in the area of no blood perfusion such as necrotic center of the solid tumor. In order to get enough thermal coverage of the target volume having the significant blood perfusion the power produced by the Thermo-Brachytherapy seed needs to be increased. i.e., the heat taken out from the target by the blood perfusion can be compensated by increasing the power generated by the thermoseed. To amplify thermal power of the seed one needs to raise the value of the magnetic field parameter (frequency or field strength or both). In general the blood perfusion rate in the normal tissue is greater than the blood perfusion rate in the cancerous tissue. This effect actually works in favor of the Thermo-Brachytherapy treatment. In such case the blood perfusion in the normal tissue takes heat away from normal structures and keeps the non-cancerous tissue at the lower temperature. However in a vascular cancerous tissue less heat is taken out from the target tissue keeping the target relatively hot.

In our model phantom, a relatively small target size was selected to allow for quicker simulation times thus allowing calculations for a set of different parameter combinations to be conducted. The model still demonstrates the essential trends and heat patterns achievable in a larger phantom with more seeds.

Conclusions

The proposed Thermo-Brachytherapy seed requires only small changes in the internal structure of a standard commercial brachytherapy seed model to gain heating capability. This modification only slightly changes radiation characterizing parameters. The Thermo-Brachytherapy seed serves as a single source of concurrent radiation and heat. It also acts as a self regulating thermal source and does not require extensive invasive thermometry. The isothermal distribution within the target volume to match with the prescribed radiation isodose distribution for the seed configuration can be achieved by changing frequency and

intensity of the alternating applied magnetic field. In case of the tissue with the significant blood perfusion the blood flow alters the thermal distribution within the target tissue. The effect of the blood perfusion could be compensated by adjusting the externally applied magnetic field parameters.

Conflict of Interest: None

Acknowledgements

This project is partially supported with an STTR grant from the NIH, 10-2011.

References

- Habash RWY, Bansal R, Krewski D, Alhafid HT. Thermal Therapy, Part 2: Hyperthermia Techniques. *Crit Rev Biomed Eng.* 2006;34(6):491–542
- Goldstein LS, Dewhirst MW, Repacholi M, Kheifets L. Summary, conclusions and recommendations: adverse temperature levels in the human body. *Int J Hyperthermia.* 2003;19(3), 373–384 .
- Lv YG, Deng ZS, Liu J.3-D numerical study on the induced heating effects of embedded micro/nano-particles on human body subject to external medical electromagnetic field. *IEEE Trans on Nanobioscience,* 2005;4(4):284-294
- LeVeen HH, Wapnick S, Piccone V, Falk G, Ahmed Nafis. Tumor eradication by radiofrequency therapy. *JAMA.* 1976; 235(20):2198-200.
- Doss JD. Use of RF fields produce hyperthermia in animal tumors. in Proc. Int. Symp. Cancer Therapy by Hyperthermia and Radiation, 1975, pp. 226–227.
- Lehmann JF, Guy AW, Warren CG, DeLateur BJ, Stonebridge JB. Evaluation of a microwave contact applicator. *Arch Phys Med Rehabil.* 1970;51(3):143–146,.
- Marmor JB, Pounds D, Postic TB, Hahn GM. Treatment of superficial human neoplasms by hyperthermia induced by ultrasound. *Cancer* 1979;43(1):188–197.
- Takahashi H, Suda T, Motoyama H, Uzuka T, *et al.* Radiofrequency interstitial hyperthermia of malignant brain tumors: Development of heating system. *J Experimental Oncology.* 2000;22:186-190.
- Lagendijk JJW. Hyperthermia treatment planning, Tropical Review. *Phys Med Biol.* 2000; 45(5): R61-R76.
- Moroz P, Jones SK, Gray BN. Magnetically mediated hyperthermia: current status and future directions. *Int J Hyperthermia.* 2002;18(4):267-284.
- Cetas TC, Gross EJ, Contractor Y.A Ferrite Core/ Metallic Sheath Thermoseed for Interstitial Thermal Therapies. *IEEE Trans Biomed Engin.* 1998;45(1):68-77.
- van der Zee J. Heating the patient: a promising approach?. *Ann Oncol.* 2002;13(8);1173-1184.
- Wust P, Hildebrandt B, Sreenivasa G, *et al.* Hyperthermia in combined treatment of cancer. *Lancet Oncol.* 2002;3(8):487-497.
- Deger S, Taymoorian K, Boehmer D, *et al.* Thermoradiotherapy Using Interstitial Self-Regulating Thermoseeds: An Intermediate Analysis of a Phase II Trial. *Eur Urol.* 2004;45(5):574–580.
- Kobayashi T, Tanaka T, Kida Y, Matsui M, Ikeda T. Interstitial hyperthermia of experimental brain tumor using implant heating system. *J Neurooncol.* 1989;7(2): 201-208.
- Steeves RA, Tompkins DT, Nash RN, *et al.* Thermo-radiotherapy of Intraocular Tumors in an Animal Model: Concurrent vs Sequential Brachytherapy and Ferromagnetic Hyperthermia. *Int J Radiat Oncol Biol Phys.*1995;33(3):659-662.
- Tubiana M, Dutreix J, Wambersie A. (Translated by Bewley DR), Introduction to Radiobiology. Taylor & Francis, London .1990
- RSICC Computer Code Collection, Monte Carlo N-Particle Transport Code System (Los Alamos National Laboratory, Los Alamos,) NM, 2000.
- Rivard MJ, Coursey BM, DeWerd LA, *et al.* Update of AAPM Task Group No. 43 Report: A revised AAPM protocol for brachytherapy dose calculations. *Med Phys.* 2004; 31(3):633-674.
- Melhus CS, Rivard MJ. Approaches to calculating AAPM TG-43 brachytherapy dosimetry parameters for ¹³⁷Cs, ¹²⁵I, ¹⁹²Ir, ¹⁰³Pd, and ¹⁶⁹Yb sources. *Med Phys.* 2006;33(6):1729–1737.
- Rivard MJ, Coursey BM, DeWerd LA, *et al.* Update of AAPM Task Group No. 43 Report: A revised AAPM protocol for brachytherapy dose calculations. *Med Phys.* 2004; 31(3):633-674.(repeated)
- Sowards KT, Meigooni AS.A Monte Carlo evaluation of the dosimetric characteristics of the Bests Model 2301 ¹²⁵I brachytherapy source. *Appl Radiat Isot.* 2002;57(3):327–333.